Transit String Dark Energy Models in f(Q) Gravity

Dinesh Chandra Maurya ¹, Archana Dixit ², Anirudh Pradhan ³,

¹Department of Mathematics, Faculty of Sciences, IASE (Deemed to be University), Sardarshahar-331 403 (Churu), Rajsthan, India.

²Department of Mathematics, Institute of Applied Sciences and Humanities, GLA University, Mathura-281 406, Uttar Pradesh, India

³ Centre for Cosmology, Astrophysics and Space Science (CCASS), GLA University, Mathura-281 406, Uttar Pradesh, India

¹E-mail:dcmaurya563@gmail.com

²E-mail:archana.dixit@gla.ac.in

³E-mail:pradhan.anirudh@gmail.com

Abstract

In this paper, we have investigated an anisotropic cosmological model in f(Q) gravity with string fluid in LRS Bianchi type-I universe. We have considered the arbitrary function $f(Q) = Q + \alpha \sqrt{Q} + \Lambda$ where α is model free parameter and Λ is the cosmological constant. We have established a relationship between matter energy density parameter Ω_m and dark energy density parameter Ω_Λ through Hubble function using using constant equation of state parameter ω . We have made observational constraint on the model using χ^2 -test with observed Hubble datasets H_0 and SNe Ia datasets, and obtained the best fit values of cosmological parameters. We have used these best fit values in the result and discussion. We have discussed our result with cosmographic coefficients and found a transit phase dark energy model. Also, we analyzed the Om diagnostic function for anisotropic universe and found that our model is either quintessence or phantom dark energy model.

Keywords: Anisotropic Universe, f(Q)-Gravity, String-fluid, Observational Constraints, Transit universe.

PACS number: 98.80-k, 98.80.Jk, 04.50.Kd

Introduction

The observational studies in the last decade of the twentieth century confirm and support the acceleration in expansion of the universe [1]-[7]. But, the theoretical development of the accelerating cosmological models have many real issues. Although, the theory of general relativity (GR) is still the most successful fundamental theory of gravity to describe the large-scale evolution of the universe. First time, Einstein has applied GR to cosmology and found an universe model which is either collapsing or expanding. At that time, the universe was supposed to be static; there was no evidence of an accelerating or expanding universe in literature. So, Einstein added a constant in his field equation to obtain a static universe which is called as "Cosmological Constant Λ " but he removed this cosmological constant from his field equation after the Hubble discovery of the expanding universe in 1929. Einstein again added this cosmological constant to his field equation after the discovery of accelerating expanding universe in 1998 but this time, the cosmological constant Λ was added to explain the dark energy problem which is supposed to cause of acceleration in expanding universe and this model is called as Λ CDM model which well fitted with observational datasets and well explain the late-time accelerating universe. Although, this Λ -term is well fitted to explain the dark energy problem, but it has two significant problem, one is its origin in equation and second is its fine-tuning problems related to the vacuum energy scale [8]-[10]. After that many cosmologists have

tried to modify Einstein field equations and some have tried to present alternate theories of gravity, to explain this dark energy problem in the universe.

The simplest generalization of GR is the so-called f(R)-gravity proposed in [11, 12] which is obtained by replacing the ricci-scalar R by an arbitrary function of R in the Hilbert-Einstein action. The modified f(R) gravity is well-known for its successful explanation of cosmic acceleration, and also it can reproduce the whole evolution history of the universe, as well as the evolution of cosmological constant Λ -term [13, 14, 15]. In order to obtain this cosmic acceleration through modified theories of gravity, there are several techniques adopted in the literature.

The amazing thing about this supposition is that it assumes that matter fields have no impact whatsoever on gravitational interaction. To express the affine features of a manifold, however, the curvature is not the only geometric object that may be used (see references [16]-[19]). In actuality, torsion and non-metricity are the other two fundamental items connected to the connection of a metric space in addition to curvature. Torsion and non-metricity disappear in Einstein's conventional General Relativity (GR). If we accept the equivalence principle's claim that gravity has a geometrical nature, it is important to investigate the different ways that gravity can have an analogous geometry. If one takes into account a flat spacetime with a metric but asymmetric connectivity, GR is represented equivalently. Torsion is given complete control over gravity in this teleparallel formulation. On an identically flat spacetime without torsion, a third equivalent and more straightforward model of GR can be built, in which gravity is this time attributed to non-metricity. Thus, the Einstein-Hilbert action $\int \sqrt{-g}R(g)$, the teleparallel equivalent of GR $\int \sqrt{-g}T$ [20] and coincident GR $\int \sqrt{-g}Q$ [21], both of which rest on a symmetric teleparallel geometry [22], can all be used to describe the same underlying physical theory, GR. You can read more about the geometrical trinity of GR and its compact presentation in [19].

The underlying underpinning of these geometrical interpretations offers modified gravity a potential path forward. Once the appropriate scalar values are, for example, promoted to arbitrary functions thereof, the analogous formulations of GR with curvature, non-metricity and torsion, represent different possible starting points to modified gravity theories. We will concentrate on the less researched example of f(Q) theories, which was introduced for the first time in [21], because it is less investigated than modified gravity theories based on f(R) [23, 24, 25] and f(T) [26, 27, 28]. Recently J. Baltran et al. [29] have investigated various features of cosmology in f(Q) geometry, although f(Q) cosmography with energy conditions can be found in [30, 31] whereas cosmological clarifications and evolution index of matter perturbations have been examined for a polynomial functional form of f(Q) [32]. Harko et al. investigated the connection matter in f(Q) gravity by supposing a power-law function [33].

Recently, "we have studied the transit phase universe in f(Q,T) gravity [34], dark energy nature of bulk viscosity in an isotropic universe with f(Q) gravity in [35, 36, 37]". Recently, Koussour et al. [38] have studied anisotropic f(Q) gravity with bulk viscosity. In this work, we will investigate the cosmological features of f(Q)-gravity with string fluid which is not investigated in literature in f(Q)-gravity. Since,

It has also been seen that in the early stages of the universe's development, strings are more important than particles, while in the late stages, massive strings are more important. We have investigated the string cosmological models in [39, 40]. The present study is organised as follows: Sect.-1 is introductory, Sect.-2 contains basic concepts and formulation of field equations in f(Q)-gravity, the solutions of the field equations are given in sect.-3 and in sect.-4, we have made some observational constraints on the model. In sect.-5, we have obtained result and discussion. In last sect.-6 conclusions are done.

2 Field Equations in f(Q) Gravity

Consider a Palatini-style framework in which connections and metrics are treated on equal footing, such that they are independent objects and their relationships are imposed only by field equations. In this model, the space-time manifold has a metric structure that comes from the metric $g_{\mu\nu}$, while affine connections $\Gamma^{\alpha}{}_{\mu\nu}$ are returns the affine structure that reveals, how tensors are transported, that define covariant derivatives. In the group of theories that this work looks at, the non-metricity tensor is the most important thing and defined as

 $Q_{\alpha\mu\nu} = \nabla_{\alpha}g_{\mu\nu}$. Compatibility of metrics reveals connection failures. We can derive the deformation from the non-metric tensor $Q_{\alpha\mu\nu}$ as

$$L^{\alpha}{}_{\mu\nu} = \frac{1}{2} Q^{\alpha}{}_{\mu\nu} - Q_{(\mu\nu)}{}^{\alpha}, \tag{1}$$

and it estimates the advancements of the symmetric part of the full connection from the Levi-Civita connection. It will also be convenient to introduce the non-metricity conjugate defined as

$$P^{\alpha}{}_{\mu\nu} = -\frac{1}{2}L^{\alpha}{}_{\mu\nu} + \frac{1}{4}(Q^{\alpha} - \tilde{Q}^{\alpha})g_{\mu\nu} - \frac{1}{4}\delta^{\alpha}{}_{(\mu Q_{\nu})}$$
 (2)

where " $Q_{\alpha} = g^{\mu\nu}Q_{\alpha\mu\nu}$ and $\tilde{Q}_{\alpha} = g^{\mu\nu}Q_{\mu\alpha\nu}$ are two independent traces of the non-metricity tensor". Now, we will define the non-metricity scalar Q that is the most important part of this work, as

$$Q = -Q_{\alpha\mu\nu}P^{\alpha\mu\nu}. (3)$$

One can observe why we say $P^{\alpha\mu\nu}$ the non-metricity conjugate since it derived as

$$P^{\alpha\mu\nu} = -\frac{1}{2} \frac{\partial Q}{\partial Q_{\alpha\mu\nu}} \tag{4}$$

Thus, we can write the action for our model in the form of an arbitrary function of non-metricity scalar Q as below

$$S = \int d^4x \sqrt{-g} \left[-\frac{1}{2} f(Q) + L_m \right] \tag{5}$$

where the matter Lagrangian is represented by Lm. The reason for the specific selection of the non-metricity scalar and the aforementioned action is that, for the choice $f = Q/8\pi G$ [21], we recover the so-called "Symmetric Teleparallel Equivalent of GR (classically, up to a boundary term").

Now, taking variation of action (5), the metric field equations are obtained as

$$\frac{2}{\sqrt{-g}}\nabla_{\alpha}(\sqrt{-g}f_{Q}P^{\alpha}_{\mu\nu}) + \frac{1}{2}g_{\mu\nu}f + f_{Q}(P_{\mu\alpha\beta}Q_{\nu}^{\alpha\beta} - 2Q_{\alpha\beta\mu}P^{\alpha\beta}_{\nu}) = T_{\mu\nu}$$

$$\tag{6}$$

where $f_Q = \partial f/\partial Q$. This takes on an even somewhat more compact shape by rising one index.,

$$\frac{2}{\sqrt{-g}}\nabla_{\alpha}(\sqrt{-g}f_{Q}P^{\alpha\mu}_{\nu}) + \frac{1}{2}\delta^{\mu}_{\nu}f + f_{Q}P^{\mu\alpha\beta}Q_{\nu\alpha\beta} = T^{\mu}_{\nu}$$

$$\tag{7}$$

By observing that the connection's variation with respect to ξ^{α} is comparable to conducting a diffeomorphism, the connection equation of motion may be easily calculated as $\delta_{\xi}\Gamma^{\alpha}{}_{\mu\beta} = -L_{\xi}\Gamma^{\alpha}{}_{\mu\beta} = -\nabla_{\mu}\nabla_{\beta}\xi^{\alpha}$, the connection is torsion-free and in the location where we have utilised it. Therefore, the connection field equations read as follows in the absence of hypermomentum.

$$\nabla_{\mu}\nabla_{\nu}(\sqrt{-g}f_{Q}P^{\mu\nu}{}_{\alpha}) = 0 \tag{8}$$

One may confirm that " $D_{\mu}T^{\mu}_{\ \nu}=0$, where D_{μ} is the metric-covariant derivative [41]", exists from the metric and connection equations, as it should due to diffeomorphism (Diff) invariance. The divergence of the energy-momentum tensor and the hypermomentum would be related in the most general case with a nontrivial hypermomentum, as shown in reference [33].

Recently, we built dark energy models in a flat FLRW universe with bulk viscosity in f(Q)-gravity (see references [35, 36, 37]), and in this study, we will derive a string-fluid dark energy model with any function $f(Q) = Q + \alpha \sqrt{Q} + \Lambda$ in LRS Bianchi Type-I space-time metric:

$$ds^{2} = A(t)^{2}dx^{2} + B(t)^{2}(dy^{2} + dz^{2}) - dt^{2}$$
(9)

Here, A(t) and B(t) are functions of cosmic time t and are referred to as metric coefficients. The non-metricity scalar Q for the line element (9) is calculated as

$$Q = 4\frac{\dot{A}}{A}\frac{\dot{B}}{B} + 2\left(\frac{\dot{B}}{B}\right)^2 \tag{10}$$

For a string-fluid, the stress-energy-momentum tensor is regarded as

$$T_{\mu\nu} = (p + \rho)u_{\mu}u_{\nu} + pg_{\mu\nu} - \lambda x_{\mu}x_{\nu}, \tag{11}$$

where $u^{\mu} = (0, 0, 0, -1)$ is the four-velocity vector in the co-moving coordinate system satisfying $u_{\mu}u^{\mu} = -x_{\mu}x^{\mu} = -1$, $u_{\mu}x^{\mu} = 0$, x^{μ} is the direction of the string and $u^{\mu}\nabla_{\nu}u_{\mu} = 0$. Here, p stands for the fluid's pressure, λ represents the string tension density, and ρ represents the energy density for the cloud of threads with attached particles. The definition of ρ_p , the particle density, is

$$\rho = \rho_p + \lambda,\tag{12}$$

where λ could be either positive or negative. [42].

In a co-moving coordinate system, we can obtain the following field equations from Eqs. (7), (9) and (11) as given below

$$f_Q \left[4\frac{\dot{A}}{A} \cdot \frac{\dot{B}}{B} + 2\left(\frac{\dot{B}}{B}\right)^2 \right] - \frac{f}{2} = \rho \tag{13}$$

$$2f_Q \left[\frac{\dot{A}}{A} \cdot \frac{\dot{B}}{B} + \left(\frac{\dot{B}}{B} \right)^2 + \frac{\ddot{B}}{B} + \right] + 2\frac{\dot{B}}{B} \dot{Q} f_{QQ} - \frac{f}{2} = -p + \lambda \tag{14}$$

$$f_Q \left[3\frac{\dot{A}}{A} \cdot \frac{\dot{B}}{B} + \left(\frac{\dot{B}}{B} \right)^2 + \frac{\ddot{A}}{A} + \frac{\ddot{B}}{B} + \right] + \left(\frac{\dot{A}}{A} + \frac{\dot{B}}{B} \right) \dot{Q} f_{QQ} - \frac{f}{2} = -p$$
 (15)

The matter conservation law is given by

$$\dot{\rho} + 3H(\rho + p) - \lambda \frac{\dot{A}}{A} = 0 \tag{16}$$

the derivative with respect to time t is represented here by the over dot symbol (·).

Now, we define the various cosmological parameters viz. volume scale-factor $V(t)=a(t)^3=AB^2$ where a(t) is the average scale-factor, the deceleration parameter $q(t)=-\frac{a\ddot{a}}{\ddot{a}^2}$ that shows the phase of the expanding universe. The mean Hubble parameter is defined as $H=\frac{1}{3}(H_x+H_y+H_z)$, with the directional Hubble parameter $H_x=\frac{\dot{A}}{A},\ H_y=H_z=\frac{\dot{B}}{B}$.

Now, we define some more geometrical parameters θ , σ^2 , Δ called as scalar expansion, shear scalar and the mean anisotropy parameter respectively and are given by

$$\theta(t) = \frac{\dot{A}}{A} + 2.\frac{\dot{B}}{B} \tag{17}$$

$$\sigma^2(t) = \frac{1}{3} \left(\frac{\dot{A}}{A} - \frac{\dot{B}}{B} \right)^2 \tag{18}$$

$$\Delta = \frac{1}{3} \sum_{i=x}^{z} \left(\frac{H_i - H}{H} \right)^2 \tag{19}$$

where H_i , i = x, y, z, are the directional Hubble parameters.

3 Solution of the field equations

Here, we have three linearly independent equations (13), (14) & (15) in five unknowns A, B, ρ , p and λ . To find exact solutions of the field equations, we have required at least two constraints on these parameters. For a spatially homogeneous metric, the normal congruence to homogeneous expansion implies that the expansion scalar θ is proportional to shear scalar σ . ie. $\sigma/\theta=k$ where k is constant. This condition leads to [43]

$$A = B^k \tag{20}$$

where k is a constant.

Secondly, we define the equation of state (EoS) for the matter as $p = \omega \rho$ and $\lambda = \omega_{\lambda} \rho$ with ω as EoS parameter for perfect fluid matter and ω_{λ} is EoS parameter for string fluid.

Now, using Eq. (20) in volume-scale factor, we get

$$A = a^{\frac{3k}{k+2}}, \quad B = a^{\frac{3}{k+2}} \tag{21}$$

Using Eq. (21) in (16) and integrating, we get the energy density ρ as

$$\rho = \rho_0 \left(\frac{a_0}{a}\right)^{3(1+\omega) - \frac{3k\omega_\lambda}{k+2}} \tag{22}$$

and using redshift relation $\frac{a_0}{a} = 1 + z$, we have

$$\rho = \rho_0 (1+z)^{3(1+\omega) - \frac{3k\omega_\lambda}{k+2}} \tag{23}$$

Now, we consider the function f(Q) as

$$f(Q) = Q + \alpha \sqrt{Q} + \Lambda \tag{24}$$

where α is model free parameter and Λ is a cosmological constant.

Now, using Eqs. (21), (23) and (24) in (13), we get

$$\Omega_m + \Omega_\Lambda = \frac{3(2k+1)}{(k+2)^2} \tag{25}$$

where $\Omega_m = \frac{\rho}{3H^2}$ and $\Omega_{\Lambda} = \frac{\Lambda}{6H^2}$, called as matter and dark energy density parameter respectively. Using Eq. (23) in (25) and taking dust-fluid $\omega = 0$, we have

$$H(t) = H_0 \frac{k+2}{\sqrt{3(2k+1)}} \sqrt{\Omega_{m0} \left(\frac{a_0}{a}\right)^{3 - \frac{3k\omega_{\lambda}}{k+2}} + \Omega_{\Lambda 0}}$$
 (26)

or

$$H(z) = H_0 \frac{k+2}{\sqrt{3(2k+1)}} \sqrt{\Omega_{m0}(1+z)^{3-\frac{3k\omega_{\lambda}}{k+2}} + \Omega_{\Lambda 0}}$$
 (27)

Now, subtracting Eq. (14) from (15) and using Eqs. (21) - (27), we get the string tension density as

$$\lambda = \frac{3H_0^2\Omega_{\Lambda 0}(k-1)(k+2)}{2k+1} + \frac{3H_0^2\Omega_{m0}(k-1)[(k+2)-k\omega_{\lambda}]}{2(2k+1)}(1+z)^{3-\frac{3k\omega_{\lambda}}{k+2}} + \frac{3\alpha H_0(k-1)(k+2)}{2\sqrt{6}(2k+1)} \times \sqrt{\Omega_{m0}(1+z)^{3-\frac{3k\omega_{\lambda}}{k+2}} + \Omega_{\Lambda 0}}$$
(28)

The deceleration parameter q is obtained as

$$q(z) = \frac{2(k^2 - k + 3)}{k + 3} - \frac{3\omega_{\lambda}(2k + 1)}{(k + 2)(k + 3)} + \frac{\alpha\sqrt{3}(k^2 - 3k + 2)}{2\sqrt{2}H_0(k + 2)(k + 3)} \frac{1}{\sqrt{\Omega_{m0}(1 + z)^{3 - \frac{3k\omega_{\lambda}}{k + 2}} + \Omega_{\Lambda0}}} - \frac{6(2 - \omega_{\lambda})(2k + 1)}{(k + 2)(k + 3)} \frac{\Omega_{\Lambda0}}{[\Omega_{m0}(1 + z)^{3 - \frac{3k\omega_{\lambda}}{k + 2}} + \Omega_{\Lambda0}]}$$
(29)

4 Observational Constraints

4.1 Hubble Parameter

In this part of the paper, we have obtain best fit curve of Hubble function as mentioned in Eq. (27), using 46 Hubble constant observed values of H(z) with error over redshift z which is obtained in [44]-[59] using differential age (DA) method time to time (see Table 1). Here, we have used χ^2 -test formula as given below:

$$\chi^2 = \sum_{i=1}^{i=N} \frac{[O_i - E_i]^2}{\sigma_i^2} \tag{30}$$

where N denotes the number of data, O_i , E_i represent the observed and estimated datasets respectively and σ_i denotes standard deviations.

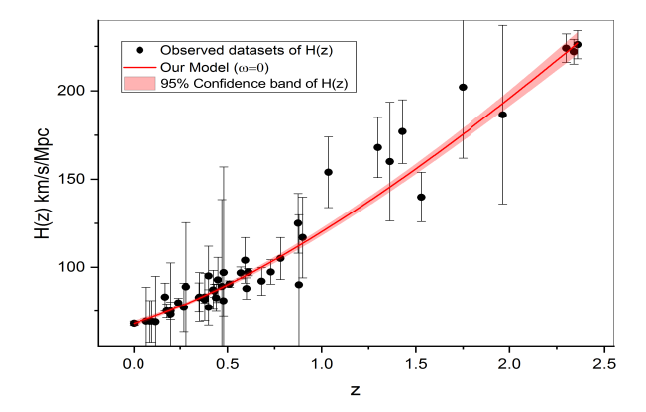


Figure 1: Best fit curve of Hubble parameter H(z) versus redshift z with H_0 data sets.

"S.No.	~	U(~)		Reference	S.No.	~	H(z)	-	Reference
	z	H(z)	σ_H			z		σ_H	
1	0	67.77	1.30	[44]	24	0.4783	80.9	9	[58]
2	0.07	69	19.6	[45]	25	0.48	97	60	[46]
3	0.09	69	12	[57]	26	0.51	90.4	1.9	[48]
4	0.10	69	12	[46]	27	0.57	96.8	3.4	[59]
5	0.12	68.6	26.2	[45]	28	0.593	104	13	[56]
6	0.17	83	8	[46]	29	0.60	87.9	6.1	[50]
7	0.179	75	4	[56]	30	0.61	97.3	2.1	[48]
8	0.1993	75	5	[56]	31	0.68	92	8	[56]
9	0.2	72.9	29.6	[45]	32	0.73	97.3	7	[50]
10	0.24	79.7	2.7	[47]	33	0.781	105	12	[56]
11	0.27	77	14	[46]	34	0.875	125	17	[56]
12	0.28	88.8	36.6	[45]	35	0.88	90	40	[46]
13	0.35	82.7	8.4	[49]	36	0.9	117	23	[46]
14	0.352	83	14	[56]	37	1.037	154	20	[47]
15	0.38	81.5	1.9	[48]	38	1.3	168	17	[46]
16	0.3802	83	13.5	[49]	39	1.363	160	33.6	[52]
17	0.4	95	17	[57]	40	1.43	177	18	[46]
18	0.004	77	10.2	[58]	41	1.53	140	14	[46]
19	0.4247	87.1	11.2	[58]	42	1.75	202	40	[52]
20	0.43	86.5	3.7	[47]	43	1.965	186.5	50.4	[47]
21	0.44	82.6	7.8	[50]	44	2.3	224	8	[55]
22	0.44497	92.8	12.9	[58]	45	2.34	222	7	53
23	0.47	89	49.6 "	[51]	46	2.36	226	8"	[54]

Table 1: Hubble's constant table.

On the basis of the minimum χ^2 , the estimated present values of various parameters are shown in the following tables.

k	Ω_{m0}	H_0	ω_{λ}	χ^2
1.5	0.36179 ± 0.04110	67.71106 ± 0.84077	0.17962 ± 0.06716	0.49955
1.2	0.36788 ± 0.04179	67.71106 ± 0.84077	0.20528 ± 0.07676	0.49955
0.9	0.36889 ± 0.04190	67.71103 ± 0.84077	0.24806 ± 0.09275	0.49955
0.6	0.36058 ± 0.04096	67.71107 ± 0.84077	0.33358 ± 0.12473	0.49955
0.3	0.33512 ± 0.03807	67.71107 ± 0.84077	0.59018 ± 0.22068	0.49955

Table 2: The best fit values of Ω_{m0} , H_0 , ω_{λ} in χ^2 -test of H(z) with H_0 data with 95% confidence level of bounds. (see Figure 1).

k	Ω	Ω_{m0}	$\Omega_{\Lambda0}$	ω_{λ}	$\rho_0 \ gm/cm^3$	$\Lambda gm/cm^3$
1.5	0.9796	0.36179 ± 0.04110	0.61781	0.17962 ± 0.06716	5.2252×10^{-36}	1.7845×10^{-35}
1.2	0.9961	0.36788 ± 0.04179	0.62822	0.20528 ± 0.07676	5.3132×10^{-36}	1.8146×10^{-35}
0.9	0.9988	0.36889 ± 0.04190	0.62991	0.24806 ± 0.09275	5.3278×10^{-36}	1.8196×10^{-35}
0.6	0.9763	0.36058 ± 0.04096	0.61572	0.33358 ± 0.12473	5.2078×10^{-36}	1.7786×10^{-35}
0.3	0.9074	0.33512 ± 0.03807	0.57228	0.59018 ± 0.22068	4.8400×10^{-36}	1.6530×10^{-35}

Table 3: The present values of energy parameters for different models.

4.2 Luminosity Distance

The redshift-luminosity distance connection is a crucial observational tool for understanding the universe's evolution. The expression for the luminosity distance (D_L) is calculated in terms of redshift because the universe's expansion causes the light emitted by distant luminous bodies to undergo a redshift. It is provided as

$$D_L = a_0 r(1+z). (31)$$

where r is the source's radial coordinate and is determined by

$$r = \int_0^r dr = \int_0^t \frac{cdt}{a(t)} = \frac{1}{a_0 H_0} \int_0^z \frac{cdz}{h(z)}$$
 (32)

where we have used $dt = dz/\dot{z}, \dot{z} = -H(1+z) \& h(z) = \frac{H}{H_0}$.

Therefore the luminosity distance is obtained as:

$$D_L = \frac{c(1+z)}{H_0} \int_0^z \frac{dz}{h(z)}$$
 (33)

4.3 Distance modulus $\mu(z)$ and Apparent Magnitude m(z)

The distance modulus μ is derived as [62]:

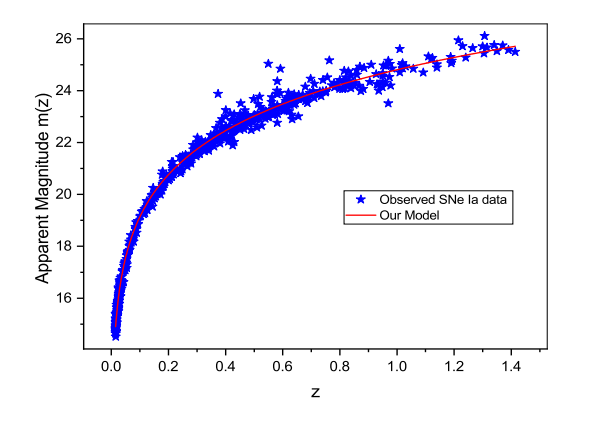
$$\mu = m_b - M
= 5log_{10} \left(\frac{D_L}{Mpc}\right) + 25
= 25 + 5log_{10} \left[\frac{c(1+z)}{H_0} \int_0^z \frac{dz}{h(z)}\right].$$
(34)

The absolute magnitude M of a supernova [63, 64] is obtained as:

$$M = 16.08 - 25 + 5\log_{10}(H_0/.026c) \tag{35}$$

Eqs. (34) and (35) produce the following expression for the apparent magnitude m(z)

$$m(z) = 16.08 + 5log_{10} \left[\frac{1+z}{.026} \int_0^z \frac{dz}{h(z)} \right].$$
 (36)



a.

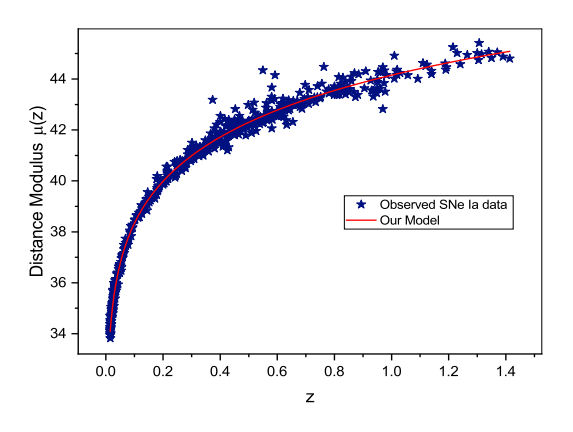


Figure 2: Best fit curve of apparent magnitude m(z) and distance modulus $\mu(z)$ over redshift z observational data sets respectively.

b.

We adopt the most recent compilation of supernovae pantheon samples which consist of 715 SN Ia data in the range of (0.01 $\leq z \leq$ 1.414) [108, 109]. For constraining various parameter of the model, we have used the following χ^2 formula:

$$\chi^{2} = \sum_{i=1}^{i=N} \frac{[O_{i} - E_{i}]^{2}}{\sigma_{i}^{2}}$$

where N denotes the number of data, O_i , E_i represent the observed and estimated datasets respectively and σ_i denotes standard deviations.

On the basis of the minimum χ^2 , the estimated present values of various parameters are shown in the following tables.

k	Ω_{m0}	ω_{λ}	χ^2
1.5	0.41233 ± 0.05648	0.19014 ± 0.05208	0.80456
1.2	0.44077 ± 0.01561	0.19781 ± 0.05962	0.80573
0.9	0.40001 ± 0.03267	0.21571 ± 0.06536	0.78481
0.6	0.43199 ± 0.02023	0.42359 ± 0.12376	0.78155
0.3	0.44022 ± 0.02063	0.60414 ± 0.13336	0.80150

Table 4: The best fit values of Ω_{m0} , ω_{λ} in χ^2 -test of apparent magnitude m(z) with SNe Ia data with 95% confidence level of bounds. (see Figure 2a).

k	Ω_{m0}	H_0	ω_{λ}	χ^2
1.5	0.29364 ± 0.06729	68.53002 ± 0.79580	0.15237 ± 0.06729	0.70864
1.2	0.27985 ± 0.01478	69.66710 ± 0.93312	0.19705 ± 0.04337	0.70869
0.9	0.28345 ± 0.02484	69.11038 ± 0.67296	0.00743 ± 0.15873	0.71542
0.6	0.32094 ± 0.02874	68.65890 ± 0.83077	0.20743 ± 0.10032	0.71568
0.3	0.27000 ± 0.02483	68.93105 ± 0.87011	0.34507 ± 0.11072	0.70231

Table 5: The best fit values of Ω_{m0} , H_0 , ω_{λ} in χ^2 -test of distance modulus $\mu(z)$ with SNe Ia data with 95% confidence level of bounds. (see Figure 2b).

5 Discussion of Results

5.1 Cosmographic Analysis

Recently, cosmography has drawn the most attention of all the rational methods (reference [65, 66]). This model-independent approach [67, 68, 69] allows the study of dark energy evolution without the requirement to select a particular cosmological model because it just uses the empirical assumptions of the cosmological principle. The typical space flight approach is based on the Taylor expansion of observations that can be directly compared to the data, and the outcomes of such operations are independent of the state equations used to research the evolution of the universe. These factors have made cosmography an effective method for dissecting the cosmological model and have led to its widespread application in attempts to comprehend the kinematics of the universe [70]-[102].

According to the cosmological principle, the sole degree of freedom that controls the cosmos is a scale factor. In order to determine the cosmographic series coefficients, such as the Hubble parameter (H), deceleration parameter (q), jerk (j), snap (s), lerk (l), and max-out (m) as described in [103], we can expand the current Taylor series of a(t) about the current time.

$$H = \frac{1}{a}\frac{da}{dt}, \quad q = -\frac{1}{aH^2}\frac{d^2a}{dt^2}, \quad j = \frac{1}{aH^3}\frac{d^3a}{dt^3}$$
(37)

and

$$s = \frac{1}{aH^4} \frac{d^4a}{dt^4}, \quad l = \frac{1}{aH^5} \frac{d^5a}{dt^5}, \quad m = \frac{1}{aH^6} \frac{d^6a}{dt^6}$$
 (38)

These values are used to explore into the dynamics of the late universe. The form of the Hubble expansion may be utilised to identify the properties of the coefficients. The sign of the parameter q in particular indicates whether the universe is expanding or reducing. Positive values of j indicate the occurrence of transitional periods when the universe's expansion varies, and the sign of j determines how the dynamics of the universe change. We also need to know the value of s in order to differentiate between evolving dark energy hypotheses and cosmological constant behaviour.

In this work, we derive these cosmographic coefficients q, j, s from the Hubble function H(z) as follows:

Deceleration Parameter

The deceleration parameter shows the phase of expansion rate of the universe and it is defined in terms of average Hubble parameter H as $q = -\frac{\dot{H}}{H^2} - 1$. The variation of q(z) over redshift z shows the different phases of the evolution of the universe, q > 0 shows deceleration, q = 0 shows phase transition and q < 0 shows acceleration in expansion. As $z \to 0$, we get the present value of q_0 . Thus, the deceleration parameter q(z) is obtained using equation (27) as follows:

$$q(z) = -1 + \frac{3\Omega_{m0}(k - k\omega_{\lambda} + 2)(1+z)^{3 - \frac{3k\omega_{\lambda}}{k+2}}}{2(k+2)\left[\Omega_{m0}(1+z)^{3 - \frac{3k\omega_{\lambda}}{k+2}} + \Omega_{\Lambda 0}\right]}.$$
(39)

The expression in Eq. (39) represents the deceleration parameter q(z) and its geometrical behaviour is shown in Figure 3a. One can see that q(z) is an increasing function of redshift z and $q \to -1$ as $z \to -1$. The present value of q is measured as $q_0 = -0.4887$ for H_0 datasets and $q_0 = -0.3855$ for SNe Ia datasets that shows that our universe model is in accelerating phase at present. At z = 0, q_0 is obtained as

$$q_0 = -1 + \frac{3\Omega_{m0}(k - k\omega_{\lambda} + 2)}{2(k+2)\left[\Omega_{m0} + \Omega_{\Lambda 0}\right]}.$$
(40)

From which, we can obtained the condition for acceleration in expansion q < 0 as

$$\Omega_{\Lambda 0} > \frac{(2k+1)(k-3k\omega_{\lambda}+2)}{(k+2)^2(k-k\omega_{\lambda}+2)}$$
(41)

For k = 1, ω_{λ} vanishes and model represents a flat Λ CDM model as $q_0 = \frac{1}{2}(1 - 3\Omega_{\Lambda})$ that reveals the condition for acceleration q < 0 when $\Omega_{\Lambda} > \frac{1}{3}$ and as $\Omega_{\Lambda} \to 1$, $q \to -1$. Also, from Figure 3a, we can see that q shows a signature-flipping (decelerating to accelerating) and hence, we have calculated the transition redshift z_t such that $q(z_t) = 0$ which is obtained as follows:

$$z_t = \left[\frac{2\Omega_{\Lambda 0}}{\Omega_{m0}} \frac{k+2}{k-3k\omega_{\lambda}+2}\right]^{\frac{k+2}{3(k-k\omega_{\lambda}+2)}} - 1 \tag{42}$$

SNe type Ia measurements offer the most conclusive empirical proof of the change from past deceleration to present acceleration. The SNe data support recent acceleration (z < 0.5) and prior deceleration (z > 0.5), according to their preliminary study. Recent results from the High-z Supernova Search (HZSNS) team include $z_t = 0.46 \pm 0.13$ at $(1;\sigma)$ c.l. [2,3,104] in 2004 and $z_t = 0.43 \pm 0.07$ at $(1;\sigma)$ c.l. [104] in 2007. The transition redshift obtained from the Supernova Legacy Survey (SNLS) by Astier et al. [105] and Davis et al. [60] is $z_t \sim 0.6$ $(1;\sigma)$, which is more in line with the flat Λ CDM model $(z_t = (2\Omega_{\Lambda}/\Omega_m)^{\frac{1}{3}} - 1 \sim 0.66)$. An additional restriction is $0.60 \le z_t \le 1.18$ $(2\sigma, \text{ joint analysis})$ [106]. Additionally, the transition redshift for our deduced model is $z_t \cong 0.7133$, 0.5271 along two datasets (see Figure 3a), which is in good accord with the Type Ia supernovae Hubble diagram, including the farthest known supernova SNI997ff at $z \approx 1.7$ (Riess et al.; Amendola; [107]). This discovery indirectly demonstrates that the transition redshift can be used to reevaluate the history of cosmic expansion.

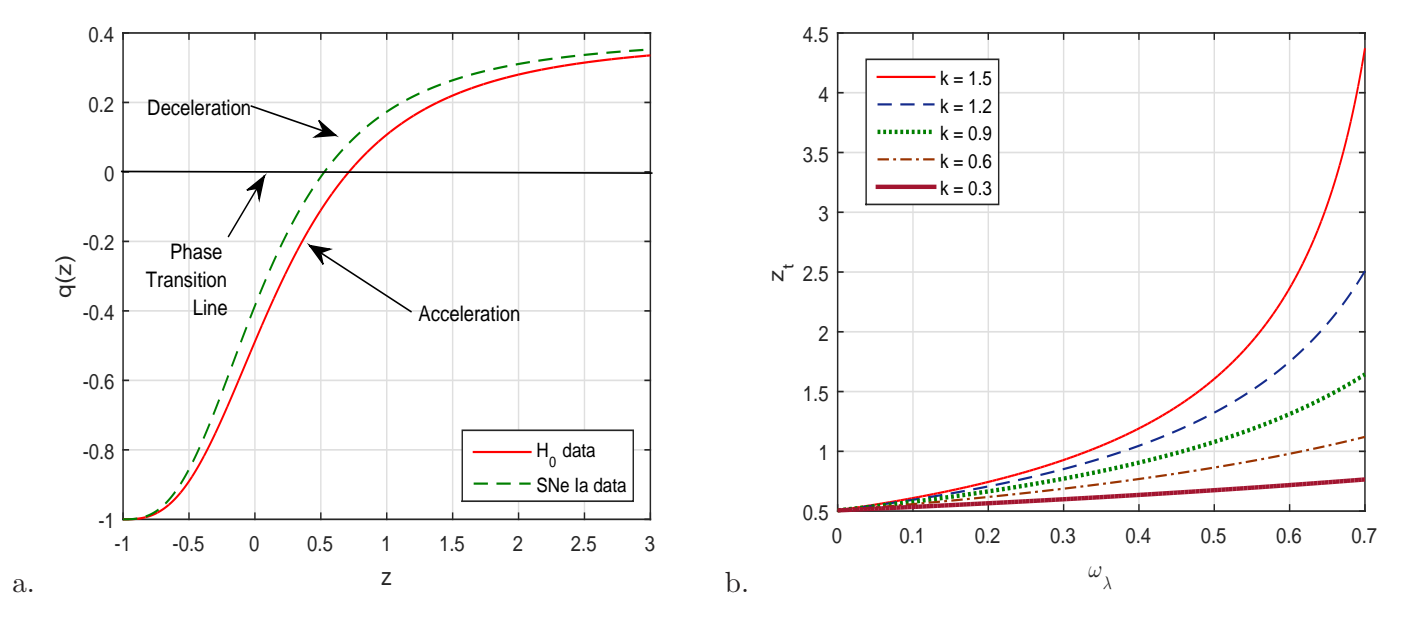


Figure 3: The behaviour of deceleration parameter q(z) over redshift z and transition redshift z over ω_{λ} respectively.

Equation (42) represents the expression for transition redshift in our model and Figure 3b shows its behaviour over ω_{λ} for different values of $0.3 \le k \le 1.5$. One can see that $z_t \to (2\Omega_{\Lambda}/\Omega_m)^{\frac{1}{3}} - 1$ as $(k, \omega_{\lambda}) \to (1, 0)$ that shows Λ CDM value.

Jerk Parameter

The third cosmographic coefficient jerk parameter is obtained as

$$j(z) = 1 - \frac{3\Omega_{m0}(k - k\omega_{\lambda} + 2)(1 + z)^{3 - \frac{3k\omega_{\lambda}}{k+2}}}{(k+2)\left[\Omega_{m0}(1+z)^{3 - \frac{3k\omega_{\lambda}}{k+2}} + \Omega_{\Lambda 0}\right]} + \frac{9\Omega_{m0}^{2}(k - k\omega_{\lambda} + 2)^{2}(1+z)^{6 - \frac{6k\omega_{\lambda}}{k+2}}}{4(k+2)^{2}\left[\Omega_{m0}(1+z)^{3 - \frac{3k\omega_{\lambda}}{k+2}} + \Omega_{\Lambda 0}\right]^{2}} + \frac{\Omega_{m0}(3k\omega_{\lambda} - 2k - 4)(3k\omega_{\lambda} - 3k - 6)(1+z)^{2 - \frac{3k\omega_{\lambda}}{k+2}}}{2(k+2)^{2}\left[\Omega_{m0}(1+z)^{3 - \frac{3k\omega_{\lambda}}{k+2}} + \Omega_{\Lambda 0}\right]} - \frac{\Omega_{m0}^{2}(3k\omega_{\lambda} - 3k - 6)^{2}(1+z)^{5 - \frac{6k\omega_{\lambda}}{k+2}}}{4(k+2)^{2}\left[\Omega_{m0}(1+z)^{3 - \frac{3k\omega_{\lambda}}{k+2}} + \Omega_{\Lambda 0}\right]^{2}}.$$

$$(43)$$

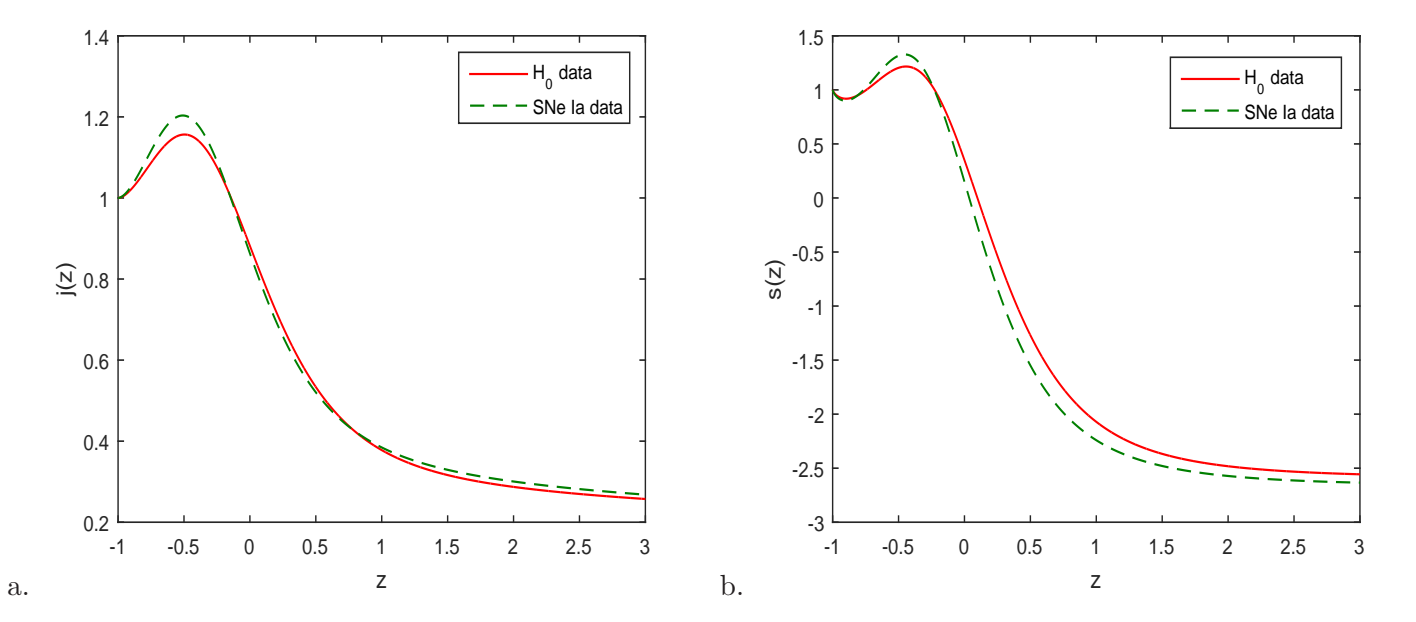


Figure 4: The variation of jerk j(z) and snap s(z) parameter over redshift z respectively.

Equation (43) shows the expression for jerk parameter j(z) and Figure 4a reveals its evolution with redshift z. One can see that it varies over (0.2, 1.4) and $j \to 1$ as $z \to -1$. Also, we can see that j > 0 over the range ($0 \le z \le 3$) that reveals the transition phase in evolution of the universe [2, 3, 60] and [104]-[107]. The present value of jerk parameter is estimated as $j_0 = 0.8819$, 0.8632 along two datasets respectively H_0 datasets and SNe Ia datasets.

Snap Parameter

The fourth cosmographic coefficient snap parameter s(z) in our model is obtained as

$$s(z) = 1 - \frac{9\Omega_{m0}(k - k\omega_{\lambda} + 2)}{2(k + 2) \left[\Omega_{m0} + \Omega_{\Lambda 0}(1 + z)^{\frac{3k\omega_{\lambda}}{k + 2} - 3}\right]} + \frac{27\Omega_{m0}^{2}(k - k\omega_{\lambda} + 2)^{2}}{4(k + 2)^{2} \left[\Omega_{m0} + \Omega_{\Lambda 0}(1 + z)^{\frac{3k\omega_{\lambda}}{k + 2} - 3}\right]^{2}}$$

$$- \frac{27\Omega_{m0}^{3}(k - k\omega_{\lambda} + 2)^{3}}{8(k + 2)^{3} \left[\Omega_{m0} + \Omega_{\Lambda 0}(1 + z)^{\frac{3k\omega_{\lambda}}{k + 2} - 3}\right]^{3}} + \frac{3\Omega_{m0}(3k\omega_{\lambda} - 2k - 4)(3k\omega_{\lambda} - 3k - 6)(1 + z)^{2 - \frac{3k\omega_{\lambda}}{k + 2}}}{2(k + 2)^{2} \left[\Omega_{m0}(1 + z)^{3 - \frac{3k\omega_{\lambda}}{k + 2}} + \Omega_{\Lambda 0}\right]}$$

$$- \frac{3\Omega_{m0}^{2}(3k\omega_{\lambda} - 3k - 6)^{2}(1 + z)^{5 - \frac{6k\omega_{\lambda}}{k + 2}}}{4(k + 2)^{2} \left[\Omega_{m0}(1 + z)^{3 - \frac{3k\omega_{\lambda}}{k + 2}} + \Omega_{\Lambda 0}\right]}^{2} - \frac{\Omega_{m0}(3k\omega_{\lambda} - 2k - 4)(3k\omega_{\lambda} - 3k - 6)(1 + z)^{3 - \frac{3k\omega_{\lambda}}{k + 2}}}}{2(k + 2)^{2} \left[\Omega_{m0}(1 + z)^{3 - \frac{3k\omega_{\lambda}}{k + 2}} + \Omega_{\Lambda 0}\right]}^{2} + \frac{\Omega_{m0}^{2}(3k\omega_{\lambda} - 3k - 6)^{2}(1 + z)^{6 - \frac{6k\omega_{\lambda}}{k + 2}}}}{4(k + 2)^{2} \left[\Omega_{m0}(1 + z)^{3 - \frac{3k\omega_{\lambda}}{k + 2}} + \Omega_{\Lambda 0}\right]}^{3} + \frac{3\Omega_{m0}^{3}(3k\omega_{\lambda} - 3k - 6)^{3}(1 + z)^{7 - \frac{9k\omega_{\lambda}}{k + 2}}}}{8(k + 2)^{3} \left[\Omega_{m0}(1 + z)^{3 - \frac{3k\omega_{\lambda}}{k + 2}} + \Omega_{\Lambda 0}\right]^{3}} + \frac{3\Omega_{m0}^{3}(3k\omega_{\lambda} - 3k - 6)^{2}(3k\omega_{\lambda} - 2k - 4)(1 + z)^{4 - \frac{3k\omega_{\lambda}}{k + 2}}}}{4(k + 2)^{3} \left[\Omega_{m0}(1 + z)^{3 - \frac{3k\omega_{\lambda}}{k + 2}} + \Omega_{\Lambda 0}\right]^{2}} + \frac{\Omega_{0}(3k\omega_{\lambda} - 3k - 6)^{2}(3k\omega_{\lambda} - 2k - 4)(3k\omega_{\lambda} - 3k - 6)(1 + z)^{4 - \frac{3k\omega_{\lambda}}{k + 2}}}}{2(k + 2)^{3} \left[\Omega_{m0}(1 + z)^{3 - \frac{3k\omega_{\lambda}}{k + 2}} + \Omega_{\Lambda 0}\right]^{\frac{1}{2}}} - \frac{9\Omega_{m0}^{3}(3k\omega_{\lambda} - 3k - 6)^{2}(3k\omega_{\lambda} - 2k - 4)(3k\omega_{\lambda} - 3k - 6)(1 + z)^{4 - \frac{3k\omega_{\lambda}}{k + 2}}}}{2(k + 2)^{3} \left[\Omega_{m0}(1 + z)^{3 - \frac{3k\omega_{\lambda}}{k + 2}} + \Omega_{\Lambda 0}\right]^{\frac{1}{2}}} - \frac{9\Omega_{m0}^{3}(3k\omega_{\lambda} - 3k - 6)^{2}(3k\omega_{\lambda} - 2k - 4)(3k\omega_{\lambda} - 3k - 6)(1 + z)^{4 - \frac{3k\omega_{\lambda}}{k + 2}}}}{2(k + 2)^{3} \left[\Omega_{m0}(1 + z)^{3 - \frac{3k\omega_{\lambda}}{k + 2}} + \Omega_{\Lambda 0}\right]^{\frac{1}{2}}}} - \frac{9\Omega_{m0}^{3}(3k\omega_{\lambda} - 3k - 6)^{2}(3k\omega_{\lambda} - 3k - 6)(1 + z)^{4 - \frac{3k\omega_{\lambda}}{k + 2}}}}{2(k + 2)^{3} \left[\Omega_{m0}(1 + 2)^{3 - \frac{3k\omega_{\lambda}}{k + 2}} + \Omega_{\Lambda 0}\right]^{\frac{1}{2}}}}$$

$$- \frac{9\Omega_{m0}^{3}(k - k\omega_{\lambda} + 2)^{3}(2k +$$

Equation (44) represents the expression for snap parameter s(z) and its geometrical behaviour is shown in Figure 4b. We can see that s(z) varies as (-3, 1.5) over the range $(0 \le z \le 3)$ and as $z \to -1$, $s \to 1$ that shows the existence of dark energy in the universe [70]-[102]. The present value of snap parameter is estimated as $s_0 = 0.3500$, 0.1503 along two datasets respectively H_0 datasets and SNe Ia datasets.

5.2 Energy Density

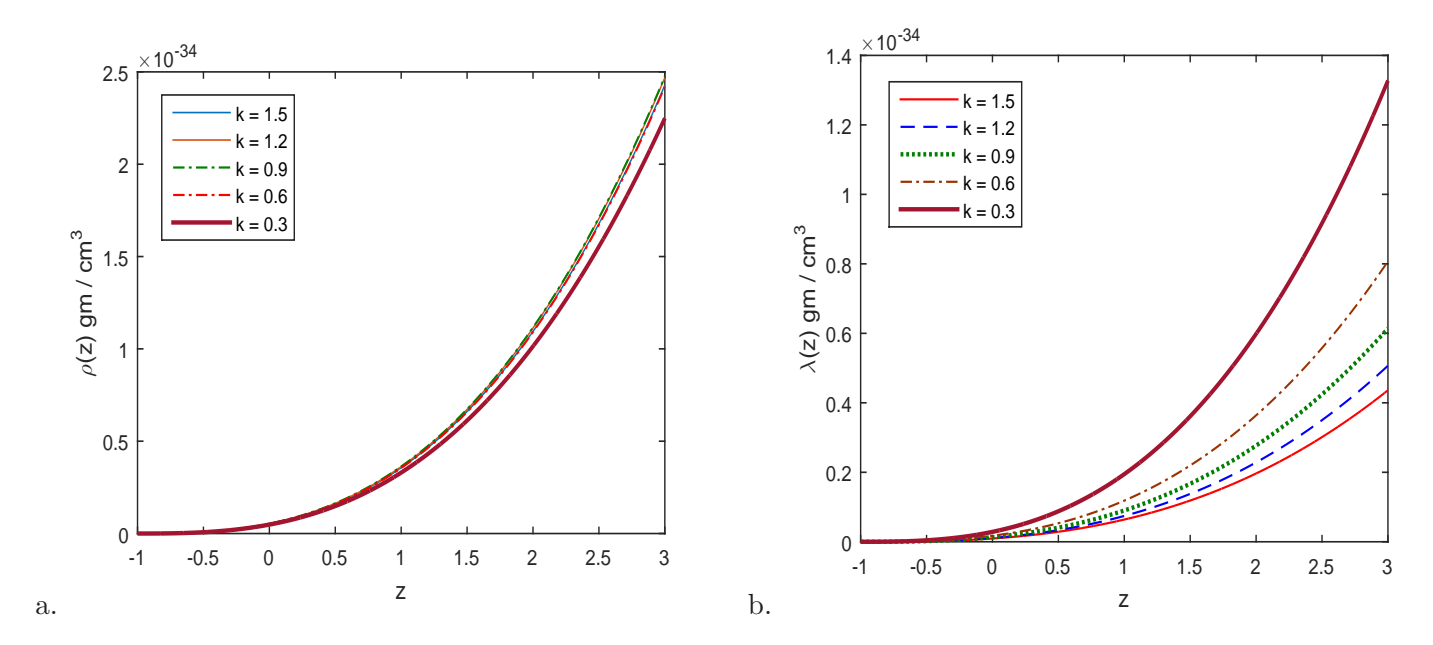


Figure 5: The behaviour of total energy density $\rho(z)$ and string tension density $\lambda(z)$ over z respectively.

Eqs. (23) & (28) represent the expressions for total energy density $\rho(z)$ and string tension density $\lambda(z)$ respectively and their geometrical behaviour are shown in Figure 5a & Figure 5b. One can see that the total energy density ρ is increasing with redshift z and as $z \to -1$, $\rho \to 0$ and as $z \to \infty$, $\rho \to \infty$. One can see that $\lambda(z)$ is an increasing function of z which shows that early universe is string dominated and with evolution of the universe it decreases to zero. From the Table 2, one can see that $\omega_{\lambda} > 0$ which shows that $\lambda > 0$ as given in [42, 43]. Reduction in string tension density causes the acceleration in expansion of the universe. We can see that the particle energy density $\rho_p > 0$ or $\rho - \lambda > 0$ i.e. all energy conditions are satisfied.

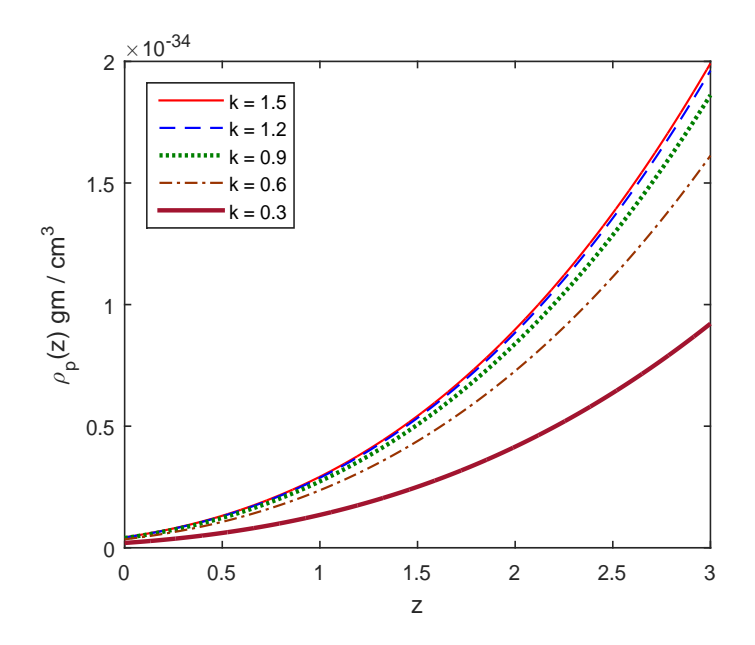


Figure 6: The variation of particle energy density ρ_p with redshift z.

The energy density parameters Ω_m and Ω_{Λ} are given by Eq. (25) and their geometrical behaviour are shown

in the figures 7a & 7b. One can see that matter energy density parameter Ω_m is an increasing function of z that shows early universe is matter dominated and the dark energy density parameter Ω_{Λ} is a decreasing function of redshift z and $\Omega_{\Lambda} \to 1$ as z tends to minus one that shows late-time universe is dark energy dominated. From the Table 3, one can see that the total energy density parameter $\Omega < 1$ that shows our universe model is closed universe and it tends to flat $\Omega \to 1$ that shows late-time universe tends to Λ CDM model.

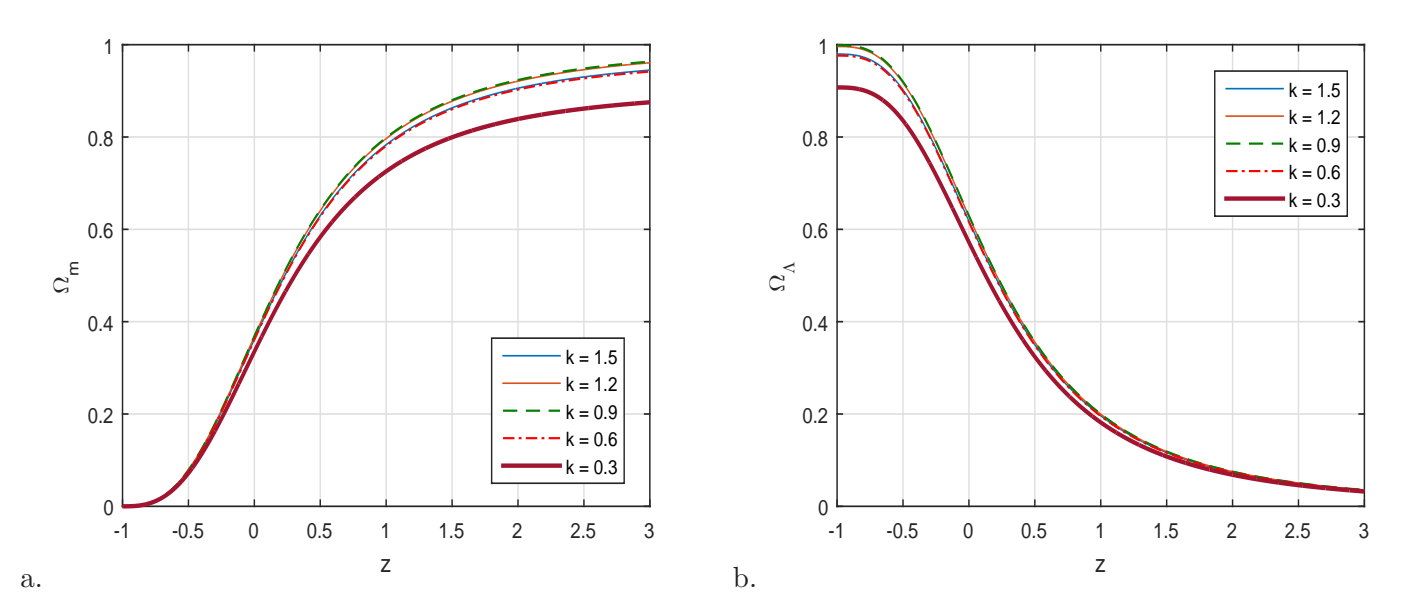


Figure 7: The variation of energy density parameters Ω_m and Ω_{Λ} with redshift z respectively.

5.3 Om Diagnostic Analysis

The cosmic dark energy models can be classified through behaviour of Om diagnostic function [61]. The diagnostic for a spatially homogeneous and anisotropic universe is given by

$$Om_i = \frac{\left(\frac{H_i(z)}{H_0}\right)^2 - 1}{(1+z)^3 - 1}, \quad i = x, y, z.$$
(45)

where $H_x = \frac{3k}{k+2}H(z)$ and $H_y = H_z = \frac{3}{k+2}H(z)$ Hubble parameters along three axes and H(z) is the average Hubble parameter given in Eq. (27) and H_0 is its current value. A negative slope of Om(z) corresponds to quintessence motion, and a positive slope corresponds to phantom motion. The Om(z) constant represents the Λ CDM model.

Figure 8 shows the geometrical behaviour of Om diagnostic function Om(z) over redshift z in different directions and mathematical expression is given in above equation (45). From figure 8a, one can see that the slope of Om(z) function is negative for k = 1.5, 1.2 that shows quintessence behaviour and positive for k = 0.9, 0.6, 0.3 that shows phantom behaviour of our model. Also, from figure 8b, one can see that the slope of Om(z) function is posive for k = 1.5, 1.2 that shows phantom behaviour and negative for k = 0.9, 0.6, 0.3 that shows quintessence behaviour of our model. Thus, we found that our model is either quintessence dark energy model or phantom dark energy model.

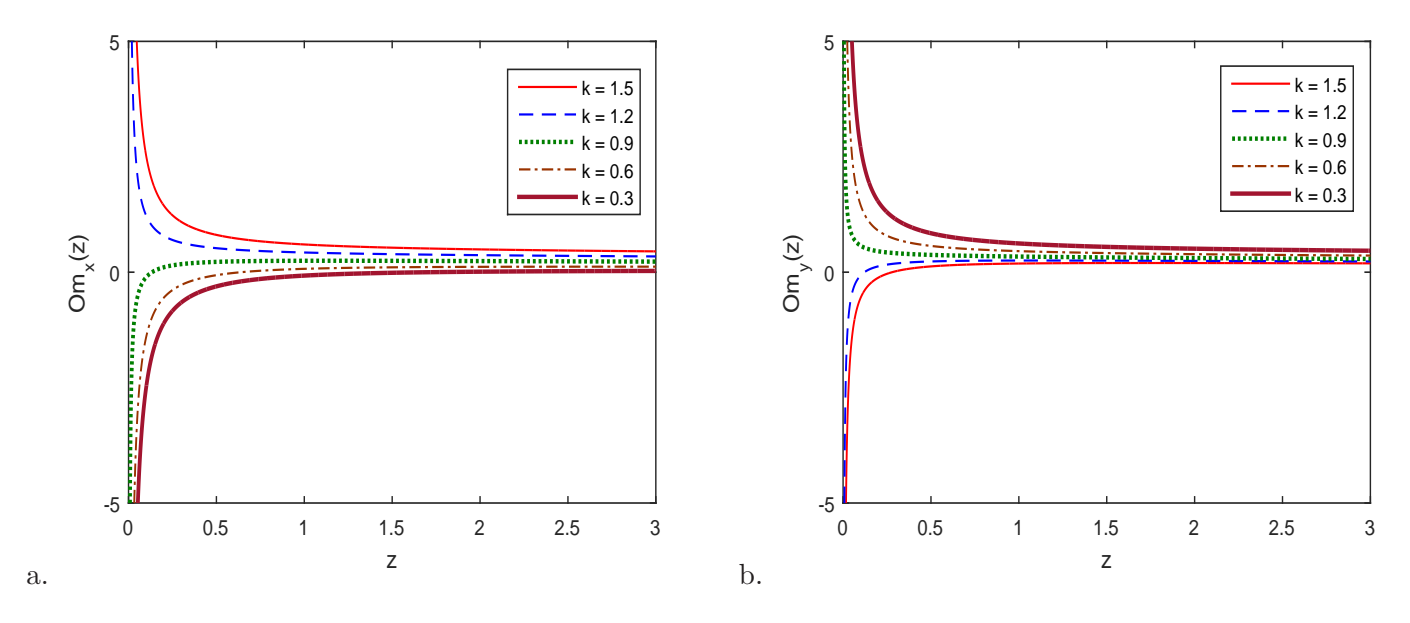


Figure 8: The variation of Om diagnostic function Om(z) over redshift z respectively in the direction of axes.

6 Conclusions

In this paper, we have investigated an anisotropic cosmological model in f(Q) gravity with string fluid in LRS Bianchi type-I universe. We have considered the arbitrary function $f(Q) = Q + \alpha \sqrt{Q} + \Lambda$ where α is model free parameter and Λ is the cosmological constant. We have established a relationship between matter energy density Ω_m and dark energy density Ω_Λ through Hubble function using using constant equation of state parameter ω, ω_λ with $p = \omega \rho$ & $\lambda = \omega_\lambda \rho$. We have made observational constraint on the model using χ^2 -test with 46 observed Hubble datasets H_0 and 715 observed datasets of SNe Ia and obtained the best fit values of cosmological parameters. We have used these best fit values to obtain the result and discussion. The estimated values of various parameters in our model is given in the following Table 6:

Parameters	H_0	SNe Ia
k	1.2	1.2
Ω	0.9961	0.9961
Ω_{m0}	0.36788	0.44077
$\Omega_{\Lambda0}$	0.62822	0.55533
ω_{λ}	0.20528	0.19781
H_0	67.71106	69.66710
$ ho_0$	5.3132×10^{-36}	6.7653×10^{-36}
Λ	1.8146×10^{-35}	1.7047×10^{-35}
α	1462.0	2414.9
q_0	-0.4887	-0.3855
j_0	0.8819	0.8632
s_0	0.3500	0.1503
z_t	0.7133	0.5271

Table 6: The estimated values of various cosmological parameters in our model.

The main features of our derived model are as follows:

• The present model shows a signature-flipping (decelerating to accelerating) point at $z_t = 0.7133, 0.5271$

respectively for two datasets which are good features of our model and it is supported by recent observations [2, 3, 60] and [104]-[107].

- We have found that the early universe is anisotropic and string dominated and decreasing string tension density may causes the acceleration in expansion.
- The total energy density parameter $\Omega < 1$ and hence, the derived model is a closed universe model and in present $\Omega_m < \Omega_{\Lambda}$ that shows that the present universe is dark energy dominated.
- We have found the present value of cosmographic coefficients $H_0 = 67.71106$, 69.66710 Km/s/Mpc, deceleration parameter $q_0 < 0$ and jerk parameter $j_0 > 0$ and so, the present phase of our universe model is accelerating. The positive signature of jerk parameter j > 0 supported the phase transition in our universe model. The values snap parameter (-3, 1.5) supported dark energy dominated universe.
- We have found that all the energy conditions are satisfied and we have estimated the present values of energy densities ρ_0 and ρ_p (see Table 6).
- We have analysed the Om diagnostic analysis for anisotropic universe and found that our universe is either quintessence or dark energy dominated universe model.
- We have estimated the value of model free parameter $\alpha = 1462.0$, 2414.9 respectively for two datasets H_0 and SNe Ia data.

Acknowledgement

A. Pradhan & A. Dixit thank the IUCAA, Pune, India for providing facilities under associateship programs. D.C. Maurya is thankful to IASE (Deemed to be University), GVM, Sardarshahr, Rajasthan, India to providing facilities and support where part of this work is carried out.

References

- [1] S. Perlmutter et al., Measurements of Ω and Λ from 42 high-redshift supernovae, Astrophys. J. **517** (1999) 565-586.
- [2] A. G. Riess *et al.*, Observational evidence from supernovae for an accelerating universe and a cosmological constant, *Astrphys. J.* **116** (1998) 1009-1038.
- [3] A. G. Riess *et al.*, Type-Ia supernova discoveries of $z \ge 1$ from the Hubble space telescope: Evidence from past deceleration and constraints on dark energy evolution, *Astrophys. J.* **607** (2004) 665-687.
- [4] D. N. Spergel *et al.*, First-year Wilkinson Microwave Anisotropy Probe (WMAP) observations: Determination of Cosmological parameters, *Astrophys. J. Suppl. Ser.* **148** (2003) 175-194.
- [5] T. Koivisto, D. F. Mota, Dark energy anisotropic stress and large scale structure formation, *Phys. Rev. D* **73** (2006) 083502.
- [6] S. F. Daniel, Large scale structure as a probe of gravitational slip, Phys. Rev. D 77 (2008) 103513.
- [7] S. Nadathur *et al.*, Testing Low-Redshift Cosmic Acceleration with Large-Scale Structure, *Phys. Rev. Lett.* **124** (2020) 221301.
- [8] E. J. Copeland, M. Sami, S. Tsujikawa, Dynamics of dark energy, Int. J. Mod. Phys. D 15 (2006) 1753-1935.
- [9] S. Nojiri, S. D. Odintsov, Introduction to Modified Gravity and Gravitational Alternative for Dark Energy, Int. J. Geom. Methods Mod. Phys. 4 (2007) 115-145.

- [10] S. Tsujikawa, Modified gravity models of dark energy, Lect. Notes Phys. 800 (2010) 99-145.
- [11] H. A. Buchdahl, Non-Linear Lagrangians and Cosmological Theory, Mon. Not. R. Astron. Soc. 150 (1970) 1-8.
- [12] J. D. Barrow, A. C. Ottewill, The stability of general relativistic cosmological theory, *J. Phys. A, Math. Gen.* **16** (1983) 2757.
- [13] S. Nojiri, S. D. Odintsov, Modified f(R) gravity consistent with realistic cosmology: From a matter dominated epoch to a dark energy universe, *Phys. Rev. D* **74** (2006) 086005.
- [14] E. Elizalde, D. Saez-Gomez, f(R) cosmology in the presence of a phantom fluid and its scalar-tensor counterpart: Towards a unified precision model of the evolution of the Universe, *Phys. Rev. D* **80** (2009) 044030.
- [15] N.Godani, G. C. Samanta, Traversable wormholes in f (R) gravity with constant and variable redshift functions, New Astronomy 80 (2020) 101399.
- [16] E. Schrodinger, E. Schrodinger, and E. Dinger, Space-Time Structure, Cambridge Science Classics (Cambridge University Press, 1985).
- [17] G. J. Olmo, Palatini approach to modified gravity: f(R) theories and beyond, Int. J. Mod. Phys. D **20** (2011) 413-462, arXiv:1101.3864 [gr-qc].
- [18] L. Heisenberg, A systematic approach to generalisations of General Relativity and their cosmological implications, *Phys. Rept.* **796** (2019) 1-113, arXiv:1807.01725 [gr-qc].
- [19] J. Beltran Jimenez, L. Heisenberg, and T. S. Koivisto, The geometrical trinity of gravity, *Universe* 5 (2019) 173, arXiv:1903.06830 [hep-th].
- [20] R. Aldrovandi and J. G. Pereira, Teleparallel Gravity, Vol. 173 (Springer, Dordrecht, 2013).
- [21] J. Beltran Jimenez, L. Heisenberg, and T. Koivisto, Coincident general relativity, *Phys. Rev. D* **98** (2018) 044048, arXiv:1710.03116 [grqc].
- [22] J. M. Nester and H. J. Yo, Symmetric teleparallel general relativity, Chin. J. Phys. 37 (1999) 113-117, arXiv:gr-qc/9809049 [gr-qc].
- [23] A. A. Starobinsky, Disappearing cosmological constant in f(R) gravity, JETP Lett. 86 (2007) 157-163, arXiv:0706.2041 [astro-ph].
- [24] L. Amendola, K. Enqvist, and T. Koivisto, Unifying Einstein and Palatini gravities, *Phys. Rev. D* 83 (2011) 044016, arXiv:1010.4776 [gr-qc].
- [25] S. Capozziello and M. De Laurentis, Extended theories of gravity, *Phys. Rept.* **509** (2011) 167-321, arXiv:1108.6266 [gr-qc].
- [26] R. Ferraro and F. Fiorini, Modified teleparallel gravity: inflation without an inflaton, *Phys. Rev. D* **75** (2007) 084031, arXiv:gr-qc/0610067 [gr-qc].
- [27] R. Ferraro and F. Fiorini, Non-trivial frames for f(T) theories of gravity and beyond, *Phys. Lett. B* **702** (2011) 75-80, arXiv:1103.0824 [gr-qc].
- [28] M. Hohmann, L. Jarv, M. Krssak, and C. Pfeifer, Modified teleparallel theories of gravity in symmetric spacetimes, *Phys. Rev. D* **100** (2019) 084002, arXiv:1901.05472 [gr-qc].
- [29] J. Beltran Jimenez, L. Heisenberg, T. S. Koivisto and S. Pekar, Cosmology in f(Q) geometry, *Phys. Rev. D* **101** (2020) 103507.

- [30] S. Mandal et al., Cosmography in f(Q) gravity, Phys. Rev. D 102 (2020) 124029.
- [31] U. k. Sharma, Shweta, & A. K. Mishra, Traversable wormhole solutions with non-exotic fluid in framework of f (Q) gravity, Int. J. Geom. Meth. Mod. Phys., 19(02) (2022) 2250019.
- [32] W. Khyllep, A. Paliathanasis, and J. Dutta, Cosmological solutions and growth index of matter perturbations in f(Q) gravity, *Phys. Rev. D* **103** (2021) 103521.
- [33] T. Harko et al., Coupling matter in modified f(Q) gravity, Phys. Rev. D 98 (2018) 084043. arXiv:1806.10437 [gr-qc].
- [34] N. Godani, G. C Samanta, FRW cosmology in f (Q, T) gravity, Int. J. Geom. Meth. Mod. Phys, 18(09),(2021) 2150134.
- [35] A. Pradhan, D. C. Maurya and A. Dixit, Dark energy nature of viscus universe in f(Q)-gravity with observational constraints, Int. J. Geom. Meth. Mod. Phys. 18 (08), 2150124
- [36] A. Dixit, D. C. Maurya and A. Pradhan, Phantom dark energy nature of bulk-viscosity universe in modified f(Q)-gravity, Inter. J. Geom. Meth. Mod. Phys. 19 (2022) 2250198-581.
- [37] A. Pradhan, A. Dixit and D. C. Maurya, Quintessence Behavior of an Anisotropic Bulk Viscous Cosmological Model in Modified f(Q)-Gravity, Symmetry 14 (2022) 2630.
- [38] M. Koussour, S. H. Shekh, M. Bennai, Anisotropic f(Q) gravity model with bulk viscosity, https://doi.org/10.48550/arXiv.2203.10954
- [39] D. C. Maurya, R. Zia and A. Pradhan, Anisotropic string cosmological model in Brans-Dicke theory of gravitation with time-dependent deceleration parameter, *Journal of Experimental and Theoretical Physics* 123 (2016) 617-622.
- [40] R. Zia, D. C. Maurya and A. Pradhan, Transit dark energy string cosmological models with perfect fluid in f(R,T)-gravity, International Journal of Geometric Methods in Modern Physics 15 (2018) 1850168.
- [41] J. Beltran Jimenez, L. Heisenberg, and T. S. Koivisto, Teleparallel Palatini theories, JCAP 1808, 039 (2018), arXiv:1803.10185 [gr-qc].
- [42] P. S. Letelier, String cosmologies, *Physical Review D* **28** (1983) 2414-2419; P. S. Letelier, Clouds of strings in general relativity, *Physical Review D* **20** (1979) 1294-1302.
- [43] C. B. Collins, E. N. Glass, D. A. Wilkinson, Exact Spatially Homogeneous Cosmologies, *Gen. Relativ. Gravit.* 12 (1980) 805-823.
- [44] S. Agarwal, R. K. Pandey, A. Pradhan, LRS Bianchi type II perfect fluid cosmological models in normal gauge for Lyra's manifold, *Int. J. Theor. Phys.* **50** (2011) 296-307.
- [45] V. K. Bhardwaj & A.K. Yadav, Some Bianchi type-V accelerating cosmological models in $f(R,T) = f_1(R) + f_2(T)$ formalism, Int. J. Geom. Meth. Mod. Phys, 17(10) (2020) 2050159.
- [46] E. Macaulay, et al., First cosmological results using Type Ia supernovae from the dark energy survey: measurement of the Hubble constant, Mon. Not. R. Astro. Soc. 486 (2019) 2184-2196.
- [47] C. Zhang, et al., Four new observational H(z) data from luminous red galaxies in the sloan digital sky survey data release seven, Res. Astron. Astrophys. 14 (2014) 1221-1233.
- [48] D. Stern, et al., Cosmic chronometers: constraining the equation of state of dark energy.I: H(z) measurements, J. Cosmol. Astropart. Phys. 1002 (2010) 008.

- [49] E. G. Naga, et al., Clustering of luminous red galaxies-IV: Baryon acoustic peak in the line-of-sight direction and a direct measurement of H(z), Mon. Not. R. Astro. Soc. **399** (2009) 1663-1680.
- [50] D. H Chauang, Y. Wang, Modelling the anisotropic two-point galaxy correlation function on small scales and single-probe measurements of H(z), $D_A(z)$ and f(z), $\sigma_8(z)$ from the sloan digital sky survey DR7 luminous red galaxies, Mon. Not. R. Astro. Soc. 435 (2013) 255-262.
- [51] S. Alam, et al., The clustering of galaxies in the completed SDSS-III Baryon Oscillation Spectroscopic Survey: cosmological analysis of the DR12 galaxy sample, Mon. Not. R. Astron. Soc. 470 (2017) 2617.
- [52] A. L. Ratsimbazafy, et al., Age-dating luminous red galaxies observed with the Southern African Large Telescope, Mon. Not. R. Astron. Soc. 467 (2017) 3239.
- [53] L. Anderson, et al., The clustering of galaxies in the SDSS-III Baryon oscillation Spectro-scopic Survey: baryon acoustic oscillations in the data releases 10 and 11 galaxy samples, Mon. Not. R. Astron. Soc. 441 (2014) 24.
- [54] M. Moresco, Raising the bar: new constraints on the Hubble parameter with cosmic chronometers at $z \equiv 2$, Mon. Not. R. Astron. Soc. **450** (2015) L16.
- [55] N. G. Busa, et al., Baryon acoustic oscillations in the Ly α forest of BOSS quasars, Astron. & Astrophys 552 (2013) A96.
- [56] M. Moresco, et al., Improved constraints on the expansion rate of the Universe up to $z \sim 1.1$ from the spectroscopic evolution of cosmic chronometers, J. Cosmol. Astropart. Phys. **2012** (2012) 006.
- [57] J. Simon, L. Verde, R. Jimenez, Constraints on the redshift dependence of the dark energy potential, Phys. Rev. D 71 (2005) 123001.
- [58] M. Moresco *et al.*, A 6 % measurement of the Hubble parameter at z ~ 0.45 direct evidence of the epoch of cosmic re-acceleration, *J. Cosmol. Astropart. Phys.* **05** (2016) 014.
- [59] G. F. R. Ellis, M. A. H. MacCallum, A class of homogeneous cosmological models, Commun. Math. Phys. 12 (1969) 108.
- [60] T. M. Davis, E. Mörtsell, J. Sollerman, et al., Scrutinizing exotic cosmological models using ESSENCE supernova data combined with other cosmological probes Astrophysical J. 666 (2007) 716-725.
- [61] V. Sahni, A. Shafieloo, A. A. Starobinsky, Two new diagnostics of dark energy, Phys. Rev. D 78 (2008) 103502.
- [62] E. J. Copeland, et al., Dynamics of dark energy, Int. J. Mod. Phys. D 15 (2006) 1753.
- [63] G. K. Goswami, R. N. Dewangan and A. K. Yadav, Astrophys. Space Sci. 361, 119 (2016).
- [64] G. K. Goswami, R. N. Dewangan, A. K. Yadav and A. Pradhan, Astrophys. Space Sci. 361, 47 (2016).
- [65] M. Visser, Cosmography: Cosmology without the Einstein equations, Gen. Rel. Grav. 37 (2005) 1541; M. Visser, Conformally Friedmann-Lemaitre-Robertson-Walker cosmologies, Class. Quant. Grav. 32 (2015) 135007.
- [66] P. K. S. Dunsby and O. Luongo, On the theory and applications of modern cosmography, Int. J. Geom. Meth. Mod. Phys. 13 (2016) 1630002.
- [67] E. R. Harrison, Observational tests in cosmology, Nature 260 (1976) 591.
- [68] O. Luongo, Dark energy from a positive jerk parameter, Phys. Lett. A 28 (2013) 1350080.

- [69] S. Capozziello, M. De Laurentis, O. Luongo and A. C. Ruggeri, Cosmographic constraints and cosmic fluids, Galaxies 1 (2013) 216.
- [70] A. Mukherjee, N. Paul and H. K. Jassal, Constraining the dark energy statefinder hierarchy in a kinematic approach, J. Cosm. Astrop. Phys. 1901 (2019) 005.
- [71] S. Capozziello, O. Farooq, O. Luongo and B. Ratra, Cosmographic bounds on the cosmological deceleration-acceleration transition redshift in f(R) gravity, Phys. Rev D **90** (2014) 044016.
- [72] A. Aviles, A. Bravetti, S. Capozziello and O. Luongo, Updated constraints on f(R) gravity from cosmography, *Phys. Rev. D* 87 (2013) 044012.
- [73] S. Capozziello, M. De Laurentis and O. Luongo, Connecting early and late universe by f(R) gravity, Int. J. Mod. Phys. D 24 (2015) 1541002.
- [74] S. Capozziello and O. Luongo, Information entropy and dark energy evolution, *Int. J. Mod. Phys. D* 27 (2018) 1850029.
- [75] O. Luongo and H. Quevedo, Cosmographic study of the universe's specific heat: a landscape for Cosmology?, Gen. Rel. Grav. 46 (2014) 1649.
- [76] H. Velten, S. Gomes and V. C. Busti, Gauging the cosmic acceleration with recent type Ia supernovae data sets, *Phys. Rev. D* **97** (2018) 083516.
- [77] U. Andrade, C. A. P. Bengaly, J. S. Alcaniz and B. Santos, Isotropy of low redshift type Ia supernovae: A Bayesian analysis, Phys. Rev. D 97 (2018) 083518.
- [78] C. Rodrigues Filho, Edesio M. Barboza, Constraints on kinematic parameters at $z \neq 0$, J. Cosm. Astrop. Phys. **1807** (2018) 037.
- [79] O. Luongo, G. B. Pisani and A. Troisi, Cosmological degeneracy versus cosmography: A cosmographic dark energy model, *Int. J. Mod. Phys. D* **26** (2017) 1750015.
- [80] Yin, ZY., Wei, H., Observational constraints on growth index with cosmography, Eur. Phys. J. C 79 (2019) 698. https://doi.org/10.1140/epjc/s1005201971918
- [81] A. Al Mamon and K. Bamba, Observational constraints on the jerk parameter with the data of the Hubble parameter, Eur. Phys. J. C 78 (2018) 862.
- [82] A. Piloyan, S. Pavluchenko and L. Amendola, Limits on the Reconstruction of a Single Dark Energy Scalar Field Potential from SNe Ia Data, *Particles* 1 (2018) 23.
- [83] F. Montanari and S. Rasanen, Backreaction and FRW consistency conditions, *J. Cosm. Astrop. Phys.* **1711** (2017) 032.
- [84] X. B. Zou, H. K. Deng, Z. Y Yin and H. Wei, Model-independent constraints on Lorentz invariance violation via the cosmographic approach, *Phys. Lett. B* **776** (2018) 284.
- [85] W. Yang, L. Xu, H. Li, Y. Wu and J. Lu, Testing the Interacting Dark Energy Model with Cosmic Microwave Background Anisotropy and Observational Hubble Data, *Entropy* **19** (2017) 327.
- [86] C. S. Carvalho, S. Basilakos, Angular distribution of cosmological parameters as a probe of inhomogeneities: a kinematic parametrisation, *Astron. Astrophys.* **592** (2016) A152.
- [87] O. Luongo, H. Quevedo, Self-accelerated Universe Induced by Repulsive Effects as an Alternative to Dark Energy and Modified Gravities, Found Phys 48 (2018) 17-26. https://doi.org/10.1007/s1070101701250

- [88] I. Semiz and A. K. Camlibel, What do the cosmological supernova data really tell us? *J. Cosm. Astrop. Phys.* **1512** (2015) 038.
- [89] Y. L. Bolotin, V. A. Cherkaski and O. A. Lemets, New cosmographic constraints on the dark energy and dark matter coupling, Int. J. Mod. Phys. D 25 (2016) 1650056.
- [90] B. Bochner, D. Pappas, M. Dong, Testing lambda and the limits of cosmography with the Union 2.1 Supernova Compilation, *Astrophys. J.* **814** (2015) 7.
- [91] S. Nesseris and J. Garcia-Bellido, Comparative analysis of model-independent methods for exploring the nature of dark energy, *Phys. Rev. D* 88 (2013) 063521.
- [92] O. Farooq, S. Crandall and B. Ratra, Binned Hubble parameter measurements and the cosmological deceleration-acceleration transition, *Phys. Lett. B* **726** (2013) 72.
- [93] F. A. Teppa Pannia and S. E. Perez Bergliaffa, Evolution of Vacuum Bubbles Embedde in Inhomogeneous Spacetimes, *J. Cosm. Astrop. Phys.* **1308** (2013) 030.
- [94] C. J. A. P. Martins, M. Martinelli, E. Calabrese and M. P. L. P. Ramos, Real-time cosmography with redshift derivatives, Phys. Rev. D 94 (2016) 043001.
- [95] F. Piazza and T. Schucker, Minimal cosmography, Gen. Rel. Grav. 48 (2016) 41.
- [96] K. Bamba, S. Capozziello, S. Nojiri and S. D. Odintsov, Dark energy cosmology: the equivalent description via different theoretical models and cosmography tests, *Astrop. Sp. Sci.* **342** (2012) 155.
- [97] S. Capozziello, V. F. Cardone, H. Farajollahi and A. Ravanpak, Cosmography in f(T) gravity, *Phys. Rev. D* 84 (2011) 043527.
- [98] J. C. Carvalho and J. S. Alcaniz, Cosmography and cosmic acceleration, Mon. Not. Roy. Astron. Soc. 418 (2011) 1873.
- [99] M. Bouhmadi-Lopez, S. Capozziello and V. F. Cardone, Cosmography of f(R)-brane cosmology, *Phys. Rev.* D 82 (2010) 103526.
- [100] S. Capozziello, V. F. Cardone and V. Salzano, Cosmography of f(R) gravity, Phys. Rev. D 78 (2008) 063504.
- [101] M. V. John, Cosmography, decelerating past, and cosmological models: learning the Bayesian way, *Astro-* phys. J. **630** (2005) 667.
- [102] S. Capozziello, Ruchika and A. A. Sen, Model-independent constraints on dark energy evolution from low-redshift observations, *Mon. Not. Roy. Astron. Soc.* **484** (2019) 4484.
- [103] S. Capozziello et al., Extended Gravity Cosmography, arXiv:1904.01427v1 [gr-qc], (2019).
- [104] Spurnova Serach Team collaboration (A. G. Riess et al.), New hubble space telescope discoveries of type Ia supernovae at z > 1: narrowing constraints on the early behavior of dark energy, Astrophys. J. 659 (2007) 98.
- [105] P. Astier *et al.*, The Supernova Legacy Survey: measurement of, and w from the first year data set, *Astron. Astrophys.* **447** (2006) 31-48.
- [106] J.A.S. Lima, J.F. Jesus, R.C. Santos, M.S.S. Gill, Is the transition redshift a new cosmological number?, arXiv:1205.4688v2[astro-ph.CO], (2012).
- [107] A. G. Riess *et al.*, The Farthest known supernova: Support for an accelerating universe and a glimpse of the epoch of deceleration, *Astrophys. J.* **560** (2001) 49.

- [108] A. K. Camlibel, I. Semiz and M. A. Feyizoglu, Pantheon update on a model-independent analysis of cosmological supernova data, *Class. Quantum Grav.* **37** (2020) 235001.
- [109] D. M. Scolnic *et al.*, The complete light-curve sample of spectroscopically confirmed SNe Ia from Pan-STARRS1 and cosmological constraints from the combined pantheon sample, *Astrophys. J.* **859** (2018) 101.